# Manganese-Containing Silica-Based Microporous Molecular Sieve MnS-1: Synthesis and Characterization

Nataša Novak Tušar,*[,†] Nataša Zabukovec Logar,[†] Iztok Arčon,[‡,§] Frederic Thibault-Starzyk,[||] Alenka Ristić,[†] Nevenka Rajić,[⊥] and Venčeslav Kaučič[†,#]

*National Institute of Chemistry, Hajdrihova 19, 1000 Ljubljana, Slovenia, Nova Gorica Polytechnic, Vipavska 13, 5000 Nova Gorica, Slovenia, Institute Jožef Stefan, Jamova 39, 1000 Ljubljana, Slovenia, Laboratoire Catalyse & Spectrochimie, ISMRA-CNRS, 6 Boulevard Maréchal Juin, 14050 Caen Cedex, France, Faculty of Technology and Metallurgy, University of Belgrade, Karnegijeva 4, 11000 Belgrade, Serbia, and Biotechnical Faculty, University of Ljubljana, Jamnikarjeva 101, 1000 Ljubljana, Slovenia*

*Received June 11, 2003. Revised Manuscript Received September 17, 2003*

Manganese-containing silicalite-1 (MnS-1) was synthesized hydrothermally in the presence of the structure-directing agent (template) tetraethylammonium hydroxide (TEAOH) for the first time. The highly crystalline MnS-1 crystallized from a gel with a molar composition of 2:1:1:50:25:935 $Na_2O$:$K_2O$:MnO:$SiO_2$:TEAOH:$H_2O$ at 175 °C after 3 days. The product was thermally stable up to 700 °C in air. The template-free MnS-1 was prepared by calcination at 550 °C in an oxygen flow. The incorporation of manganese into the framework sites of silicalite-1 was suggested by elemental, thermogravimetric, and cation exchange analyses. The X-ray absorption spectroscopic methods XANES and EXAFS confirmed the incorporation of $Mn^{3+}$ into a silicalite-1 framework. FT-IR spectroscopic studies of CO adsorption at 100 K on the MnS-1 revealed the Lewis acidity of the sample and the presence of both $Mn^{3+}$ and $Mn^{2+}$ cations in the structure.

## 1. Introduction

Silica-based molecular sieves possess remarkable catalytic properties and have been widely used as solid catalysts in various industrial processes ranging from petroleum refining to the synthesis of intermediates and fine chemicals.[1]

Silicalite-1 is a microporous silica-based molecular sieve[2] with a MFI topology of the tetrahedral framework.[3] The isomorphous substitution of $Si^{4+}$ ions in a silicalite-1 framework with tetra- and pentavalent ions such as $Ti^{4+}$, $V^{4+/5+}$, or $Sn^{4+}$ has been reported to result in novel molecular sieves with selective oxidation properties.[1] Titanium silicalite-1 (TS-1), vanadium silicalite-1 (VS-1), and tin silicalite-1 (SnS-1) have been shown to possess unique catalytic properties in oxidation reactions involving $H_2O_2$ as the oxidant.[4,5] The isomorphous substitution of $Si^{4+}$ ions in silicalite-1 with trivalent ions such as $Al^{3+}$, $B^{3+}$, $Fe^{3+}$, and $Ge^{3+}$ has been reported to result in high-quality inorganic membranes used for catalytic membrane reactors.[6,7]

The aluminum-containing silicalite-1 (ZSM-5) is a representative member of high-silica aluminosilicate molecular sieves (zeolites) exhibiting also considerable significance as catalytic materials.[1] Moreover, the isomorphous substitution of $Si^{4+}$ with trivalent $Cr^{3+}$ and $Mo^{3+}$ gives CrS-1 and MoS-1, chromium- and molybdenum-containing silicalite-1, respectively.[8,9] CrS-1 catalyzed the oxidation of toluene and alkenes using *tert*-butyl hydroperoxide (TBHP) as an oxidant under mild reaction conditions.[10] However, experimental evidence is presented that these reactions did not take place in the micropores or at the outer surface but were homogeneously catalyzed by a small amount of leached chromium.[11] MoS-1 catalyzed epoxidation of olefins.[9] The synthesis and characterization data which suggest the incorporation of $B^{3+}$, $As^{3+}$, $Nb^{3+}$, $Ru^{3+}$, and $Ta^{5+}$ into a silicalite-1 framework have also been reported.[12−16] Generally, trivalent metal ions isomorphously substitute

* To whom correspondence should be addressed. E-mail: natasa.novak@ki.si.
† National Institute of Chemistry.
‡ Nova Gorica Polytechnic.
§ Institute Jožef Stefan.
|| ISMRA-CNRS.
⊥ University of Belgrade.
# University of Ljubljana.

(1) Lercher, J. A.; Jentys, A. In *Handbook of Porous Solids*; Schüth, F., Sing, K. S. W., Weitkamp, J., Eds.; Wiley-VCH: Weinheim, Germany, 2002.
(2) Flanigen, E. M.; Bennett, J. M.; Grose, R. W.; Cohen, J. P.; Patton, R. L.; Kirchner, R. M.; Smith J. V. *Nature* **1978**, *271*, 512.
(3) Baerlocher, Ch.; Meier, W. M.; Olson, D. H. *Atlas of Zeolite Framework Types*; Elsevier: Amsterdam, The Netherlands, 2001.
(4) Ramaswamy, P.; Sivasanker, S. *Catal. Lett.* **1993**, *22*, 239.
(5) Mal, N. K.; Ramaswamy, P. *Appl. Catal., A* **1996**, *143*, 75.
(6) Tuan, V. A.; Falconer, J. L.; Noble, R. D. *Microporous Mesoporous Mater.* **2000**, *41*, 269.
(7) Li, S.; Tuan, V. A.; Falconer, J. L.; Noble, R. D. *Microporous Mesoporous Mater.* **2003**, *58*, 137.
(8) Chapus, T.; Tuel, A.; Ben Taarit, J.; Naccache, C. *Zeolites* **1994**, *14*, 349.
(9) Masteri-Farahani, M.; Farzaneh, F.; Ghandi, M. *J. Mol. Catal. A: Chem.* **2003**, *192*, 103.
(10) Singh, A. P.; Selvam, T. *J. Mol. Catal. A: Chem.* **1996**, *113*, 489.
(11) Lempers, H. E. B.; Sheldon, R. A. *J. Catal.* **1998**, *175*, 62.
(12) Howden, M. G. *Zeolites* **1985**, *5*, 334.
(13) Bhaumik, A.; Kumar, R. *J. Chem. Soc., Chem. Commun.* **1995**, 869.
(14) Prakash, A. M.; Kevan, L. *J. Am. Chem. Soc.* **1998**, *120*, 13148.

10.1021/cm031091c CCC: $25.00 
Published on Web 11/14/2003

silicon in the framework positions of high-silica zeolites and they do not exhibit redox behavior unless they are removed from the framework sites.[17] A recent study of $B^{3+}$ and $Ga^{3+}$ distribution in the framework of silicalite-1 using single-crystal synchrotron radiation X-ray diffraction confirmed an isomorphous substitution of both cations on silicon sites.[18]

Two synthesis procedures have been reported for the incorporation of manganese into silicalite-1.[19,20] The first procedure was carried out in a fluoride medium using tetrahalometalate[19] while the second one was based on the recrystallization of Mn(II)-exchanged magadiite into Mn−silicalite-1.[20] However, for both cases there is no direct evidence on the isomorphous substitution of $Si^{4+}$ framework sites by manganese.

This paper reports on a simple synthetic procedure that leads to the MnS-1, using for the first time tetraethylammonium hydroxide (TEAOH) as a structure-directing agent (template). X-ray and IR absorption spectroscopies gave direct evidence on the isomorphous substitution of $Si^{4+}$ framework sites by $Mn^{3+}$.

## 2. Experimental Section

**2.1. Synthesis.** MnS-1 was synthesized hydrothermally from a gel with the following molar composition: 2:1:1:50:25:935 $Na_2O$:$K_2O$:MnO:$SiO_2$:TEAOH:$H_2O$. The gel was prepared as follows: NaCl (Kemika), KCl (Kemika), and 9/10 of the required amount of silica (Cab-Osil M-5, Fluka, 99%) were successively added to the TEAOH (Merck, 20%). With use of an Ultra-Turrax T25 disperser (Janke-Kunkel), the reaction system was thoroughly blended to a homogeneous mixture each time before the addition of the next component. Then the solution of manganese acetate (Fluka, 70.5%), prepared in the totally required quantity of distilled water for the gel composition, was added dropwise. Finally, the residual amount (1/10) of silica was added. The reaction gel was blended to a homogeneous mixture using the disperser for 10 min. The resulting gel (pH = 13) was transferred to a 50-mL stainless steel Teflon-lined autoclave and heated under static conditions in an oven. After 3 days the crystallization was completed (pH decreased to 10) and the MnS-1 crystals were washed three times with distilled water and dried at 75 °C. The as-synthesized MnS-1 was turned to the template-free material by heating at 550 °C in an oxygen flow for 6 h using a heating rate of 2 °C/min. The light brown color of the as-synthesized MnS-1 changed to dark brown during the calcination. To check the presence of cation-exchangeable sites in the MnS-1, a cation-exchange reaction of the template-free MnS-1 was performed at room temperature by stirring the solid in a 1 M solution of NaCl. The solid/liquid mass ratio was 1:10.

**2.2. Characterization.** X-ray powder diffraction (XRPD) patterns of as-synthesized and template-free products were collected on a Siemens D-5000 diffractometer using Cu Kα radiation at room temperature. The XRPD data were collected in the $2\theta$ range from 5 to 55° in steps of 0.04°, with 1 s/step. Temperature-resolved XRPD patterns of the as-synthesized product in air were collected on the same diffractometer equipped with a HTK-16 high-temperature chamber. The $2\theta$ range was from 5 to 38° and the step was 0.026° with 4 s/step. The patterns were collected at selected temperatures between room temperature and 1000 °C with a heating rate of 10 °C/min.

The size and the morphology of as-synthesized and template-free crystals were studied with a scanning electron microscope JEOL JSM 5800. Elemental analysis was carried out using an EDXS (energy-dispersive X-ray spectroscopy) analysis within the LINK ISIS 300 system, attached to a scanning electron microscope JEOL JSM 5800. The C, H, and N content of as-synthesized and template-free products was determined using a Perkin-Elmer 2400 elemental analyzer. Thermal analyses of the as-synthesized product (TG-DSC) were performed on a SDT 2960 thermal analysis system (TA Instruments, Inc.). The measurements were carried out in static air with a heating rate of 10 °C/min.

X-ray absorption spectra of the template-free MnS-1 and reference samples in the energy region of the Mn K-edge were measured in transmission mode at E4 beamline of the HASYLAB synchrotron facility at DESY in Hamburg. The beamline provided a focused beam from an Au-coated torroidal mirror and a Si(111) double-crystal monochromator with about 1-eV resolution at the Mn K-edge. Harmonics were effectively eliminated by a plane Au-coated mirror, and by a slight detuning of the monochromator crystals, keeping the intensity at 60% of the rocking curve with the beam stabilization feedback control. Powder samples were prepared on multiple layers of adhesive tape. Several layers, stacked to obtain optimal attenuation above the Mn K-edge and improved homogeneity, were mounted on a sample holder in a vacuum chamber of the beamline so that during the measurements the samples were kept in a high vacuum. The Mn K-edge jump in the case of a MnS-1 absorption spectrum was 0.4, due to relatively small concentration of Mn in the sample. Reference spectra were measured under the same conditions on empty tapes without the sample. The standard stepping progression within the [−250 to 1000 eV] region of the Mn K-edge was adopted for EXAFS spectra with an integration time of 4 s/step. Exact energy calibration was established with the simultaneous absorption measurements on Mn metal.

The acidity of the template-free MnS-1 was characterized by IR spectroscopy on a Thermo Nicolet Avatar 360 spectrometer with an MCT detector, with 4-$cm^{-1}$ resolution and one-level zero-filling, on self-supporting wafers of the calcined solids (2 $cm^2$, 10−15 mg, prepared by the application of a pressure of $5 \times 10^7$ Pa for 10 min). The wafers were placed into a vacuum infrared quartz cell. The cell allows heating of the sample for in situ pretreatment and cooling in the infrared beam for low-temperature adsorption, as well as for introducing known quantities of gas into the cell. The sample was recalcined in situ at 300 °C under $10^4$ Pa of $O_2$ and further activated in situ at 450 °C under vacuum ($10^{-4}$ Pa). Acidity was measured by carbon monoxide (CO) adsorption and additionally checked by 2,6-lutidine adsorption. During the measurements CO was introduced in small doses on the activated sample cooled to 100 K. All spectra shown in Figures 11 and 12 are normalized to 10-mg wafers. The sample was compared with a reference sample of aluminum-containing silicalite-1, ZSM-5 (Si/Al = 320, ZEOCAT), which contains aluminum atoms comparable in amount to manganese atoms in MnS-1 (Si/Mn = 255). Redox behavior of MnS-1 was examined by performing the same thermal treatment under hydrogen and comparing the results of the low-temperature CO adsorption with those obtained after thermal treatment under oxygen.

## 3. Results and Discusion

**3.1. XRPD, SEM, and Elemental Analyses.** The as-synthesized MnS-1 was identified from XRPD pattern (Figure 1) as a single crystalline phase product with MFI structure.[3] The product, however, consisted of two different crystal morphologies: brown crystals in the majority and a white powder in the minority. Scanning

(15) Latham, K.; Thompsett, D.; Williams, C. D.; Round, C. I. *J. Mater. Chem.* **2000**, *10*, 1235.
(16) Ko, Y. S.; Ahn, W. S. *Microporous Mesoporous Mater.* **1999**, *30*, 283.
(17) Wichterlová, B.; Sobalik, Z.; Dědeček, J. *Appl. Catal. B* **2003**, *41*, 97.
(18) Palin, L.; Lamberti, C.; Kvick, Å.; Testa. F.; Aiello, R.; Milanesio, M.; Viterbo, D. *J. Phys. Chem. B* **2003**, *107*, 4034.
(19) Round, C. I.; Williams, C. W.; Duke, C. V. A. *Chem. Commun.* **1997**, 1849.
(20) Ko, Y.; Kim, S. J.; Kim, M. H.; Park, J. H.; Parise, J. B.; Uh, Y. S. *Microporous Mesoporous Mater.* **1999**, *30*, 213.

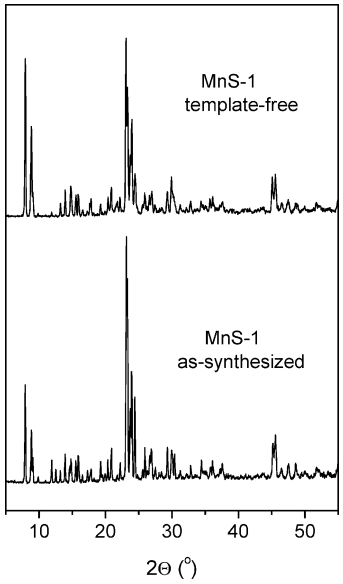


**Figure 1.** XRPD patterns of the as-synthesized and template-free MnS-1.

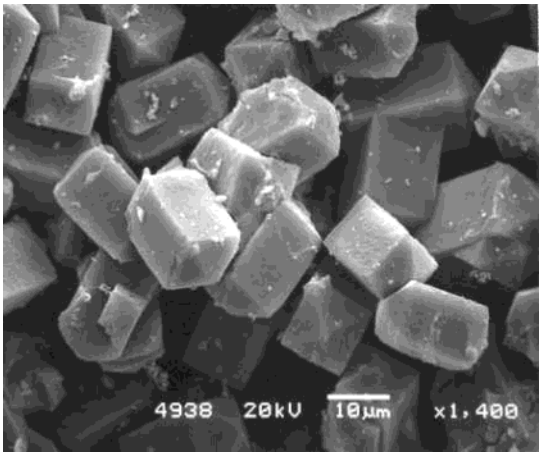


**Figure 2.** SEM photograph of the template-free material: prismatic crystals of 20 × 10 × 10 $\mu$m (brown phase) and small round crystals of less than 50 nm in size (white phase).

electron microscopy revealed that the brown phase was comprised of prismatic crystals of 20 × 10 × 10 $\mu$m (Figure 2), whereas the white one contained small round crystals of less than 50 nm in size (Figure 3). The XRPD pattern of the white phase (separated manually from the brown product) revealed that the phase was not well-crystallized, but it exhibited the same structure as the brown one (Figure 4).

Elemental analysis of the white phase of as-synthesized and template-free products gave the chemical composition corresponding to silicalite-1: [$Si_{96}O_{192}$]. From the elemental analysis of brown crystals the oxide formula was calculated to be [$Si_{95.57}Mn_{0.37}O_{192}$], suggesting that 0.4% isomorphous substitution of silicon by manganese was obtained.

**3.2.Thermogravimetric Analysis.** The TGA profile (Figure 5) of the as-synthesized MnS-1 in air shows that the desorption of water occurs up to 300 °C, whereas the decomposition of TEAOH occurs between 300 and 500 °C, in agreement with literature data.[21] The character of the mass loss (whether due to the desorption of water or to the removal of template) was determined with the aid of C, H, N analysis of the as-synthesized MnS-1. It is evident that decomposition of TEAOH occurs in two steps. This could be explained by Hofmann degradation (first step) and combustion of residue

(21) Parker L. M.; Bibby, D. M., Patterson, J. E. *Zeolites* **1984**, *4*, 168.

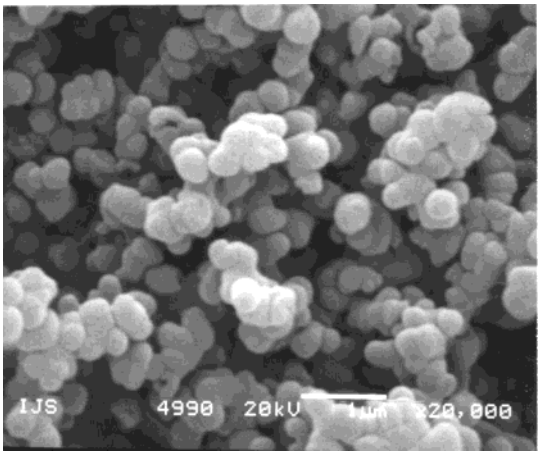


**Figure 3.** SEM photograph of the white phase: round small crystals less than 50 nm in size.

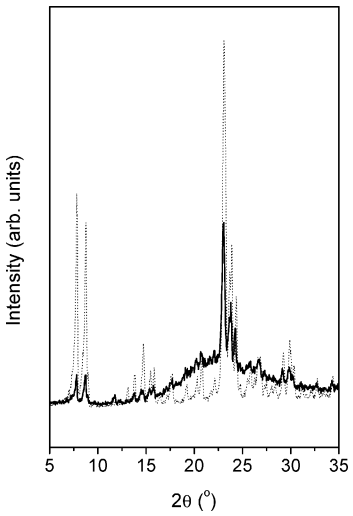


**Figure 4.** XRPD patterns of the template-free product: dotted line, brown phase; solid line, white phase.

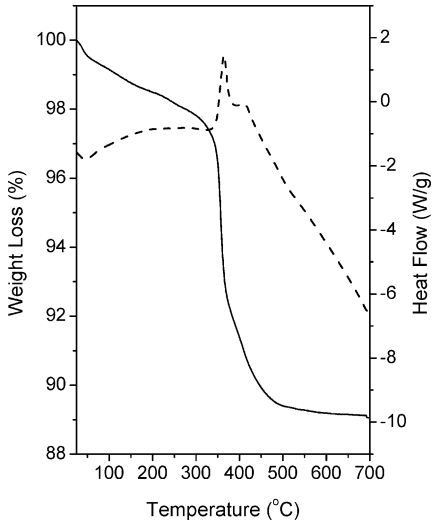


**Figure 5.** TG (solid line) and DSC (dashed line) of the as-synthesized MnS-1.

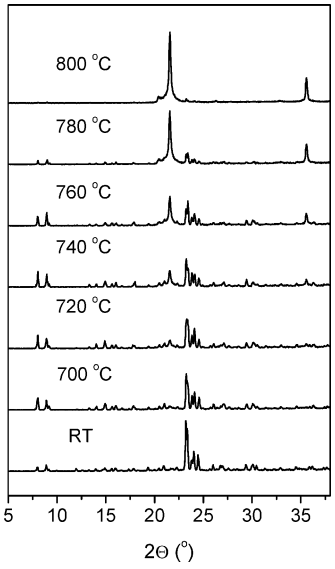


**Figure 6.** High-temperature XRPD patterns of the as-synthesized MnS-1 measured during thermal treatment in air (RT: room temperature).

(second step) or by different locations of template species inside the framework. A part of the template species in the second step may occupy the sites that are closer to the Brønsted and/or Lewis acid sites (framework manganese sites).[21,22] The DSC profile (Figure 5) exhibits an endothermic peak, indicating the desorption of water and two exotermic peaks due to the decomposition of the template.

**3.3. Structural Stability.** Thermal treatment of as-synthesized MnS-1 (Figure 6) shows that the structure is stable up to 700 °C, where it transforms to trydimite. ZSM-5 and silicalite-1 are stable up to 1000 °C.

**3.4. Exchangeable Cationic Sites in MnS-1.** A treatment of the template-free MnS-1 with NaCl solution showed that there were no exchangeable cationic sites in the framework. After cation-exchange treatment no manganese ions were found in the solution. This strongly supports the hypothesis that the manganese atoms form a constituent part of the MFI framework.

**3.5. X-ray Absorption Studies of Mn Local Environment.** The average oxidation number of manganese cations in the template-free MnS-1 sample was deduced from the energy shift of the manganese absorption edge. A linear relation between the edge shift and the oxidation state was established for the atoms with the same type of ligands.[23−25] For manganese atoms coordinated to oxygen atoms a shift of 3.5 eV per oxidation state was found.[25]

Figure 7 shows the normalized Mn XANES spectra of the template-free MnS-1 and reference manganese compounds with known oxidation numbers ($Mn^{2+}O$, $K_3[Mn^{3+}(C_2O_4)_3]\cdot 3H_2O$, and $Mn^{4+}O_2$), extracted by a standard procedure.[23] The zero energy was taken at the first inflection point of the Mn K-edge in the spectrum of Mn

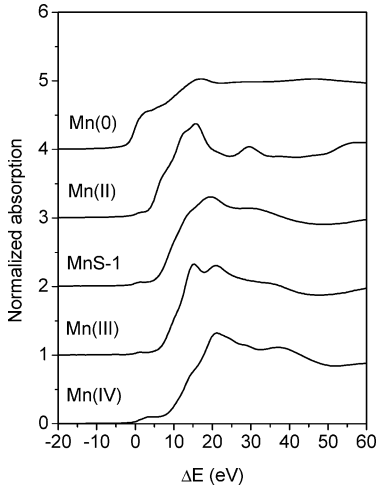


**Figure 7.** Normalized Mn K-edge XANES spectra of the template-free MnS-1 and Mn reference samples (Mn metal, $Mn^{II}O$, $K_3[Mn^{III}(C_2O_4)_3]\cdot 3H_2O$, $Mn^{IV}O_2$). The spectra are displaced vertically for clarity.

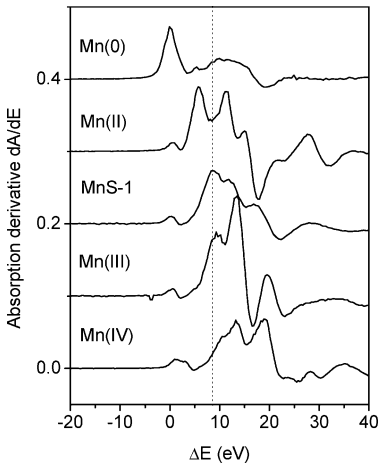


**Figure 8.** Absorption derivative of the Mn K-edge profile of the template-free MnS-1 and reference samples from Figure 7. Vertical dashed line is plotted at the energy position of Mn K-edge in the MnS-1 spectrum.

metal (6539.0 eV), that is, at the 1s ionization threshold in Mn metal. The precise energy position of the edge was taken at the edge inflection point, which can best be determined in the derivative spectrum as the tip of the first peak (Figure 8). A comparison with reference spectra shows that the edge shift in MnS-1 is the same as in $K_3[Mn^{3+}(C_2O_4)_3]\cdot 3H_2O$ compound, indicating that the average oxidation state of manganese in the MnS-1 is 3+. It is worth noticing that the presence of a smaller fraction of $Mn^{2+}$ cations in the sample is not excluded since the sensitivity of the method in determining the ratio $Mn^{2+}/Mn^{3+}$ cations is about 10%.

The Mn K-edge EXAFS spectrum of the template-free MnS-1 sample (Figure 9) was quantitatively analyzed for the coordination number, distance, and Debye−Waller factor of the nearest coordination shells of neighbor atoms. The analysis was performed with the University of Washington UWXAFS package[26] using FEFF6 code,[27] in which the photoelectron scattering

(22) Szostak R. *Handbook of Molecular Sieves*; Van Nostrand Reinhold: New York, 1992.
(23) Wong, J.; Lytle, F. W.; Messmer, R. P.; Maylotte, D. H. *Phys. Rev. B* **1984**, *30*, 5596.
(24) Arčon, I.; Mirtič, B.; Kodre, A. *J. Am. Ceram. Soc.* **1998**, *81*, 222.
(25) Ressler, T.; Brock, S. L.; Wong, J.; Suib, S. L. *J. Synchrotron Radiat.* **1999**, *6*, 728.
(26) Stern, E. A.; Newville, M.; Ravel, B.; Yacoby, Y.; Haskel, D. *Physica B* **1995**, *208−209*, 117.
(27) Rehr, J. J.; Albers, R. C.; Zabinsky, S. I. *Phys. Rev. Lett.* **1992**, *69*, 3397.

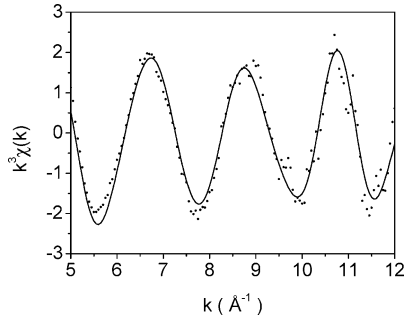


**Figure 9.** The $k^3$-weighted Mn K-edge EXAFS spectrum of the template-free MnS-1. (dots, experiment; solid line, best fit model function).

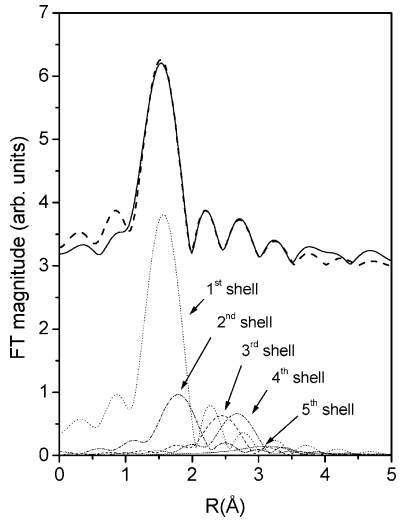


**Figure 10.** Fourier transform magnitude of the $k^3$-weighted Mn EXAFS spectrum of the template-free MnS-1, calculated in the $k$ range of 5−12 Å$^{-1}$. Above: solid line, experiment; dashed line, EXAFS model (both shifted vertically for clarity). Below: FT magnitude of consecutive neighbor shells contributions in the EXAFS model. Parameters of each shell are listed in Table 1.

paths were calculated ab initio from a presumed distribution of neighbor atoms. A Fourier-transformed $k^3$ weighted Mn EXAFS spectrum calculated in the $k$ range of 5−12 Å$^{-1}$ is shown in Figure 10 together with a best-fit EXAFS model. A very good fit in the $R$ range from 1.2 to 3.5 Å was found with three oxygen atoms in the first coordination shell, two of them at a shorter distance of 1.93 Å, and one at a longer distance of 2.15 Å. The short distance of 1.93 Å is consistent with the average tetrahedral $Mn^{3+}$−O distance of 1.93(4) Å that was found in $MnAsO_4$.[28] In the second coordination shell two oxygen atoms were found at 2.81 and 3.04 Å. Additionally, at a larger distance of about 3.5 Å a presence of silicon atoms is indicated; however, the weak signal of that neighbor shell is already hindered by the noise and the parameters could not be reliably determined. A complete list of best-fit parameters is given in Table 1.

These results of XANES and EXAFS analyses suggest that the $Mn^{3+}$ is coordinated by three lattice oxygen atoms in a distorted and coordinatively unsaturated 3-fold symmetry, which is characteristic for Lewis acid sites.

**Table 1. Structural Parameters of the Nearest Coordination Shells around Mn Atom in Template-Free MnS-1: Type of Neighbor Atom, Average Number *N*, Distance *R*, and Debye−Waller Factor $\sigma^2$ [a]**

| neighbor | *N* | *R* (Å) | $\sigma^2$ (Å$^2$) |
|---|---|---|---|
| O | 2.1(2) | 1.93(1) | 0.003(1) |
| O | 0.8(2) | 2.15(2) | 0.005(2) |
| O | 1.0(5) | 2.81(2) | 0.004(2) |
| O | 1.1(5) | 3.04(2) | 0.004(2) |
| Si | 0.9(6) | 3.52(2) | 0.020(5) |

[a] The amplitude reduction factor ($S_0^2 = 0.80$) was kept fixed during the fit. Best fit is obtained with a shift of energy origin $\Delta E_0$ of 3(2) eV. (Uncertainties in the last digit are given in parentheses.)

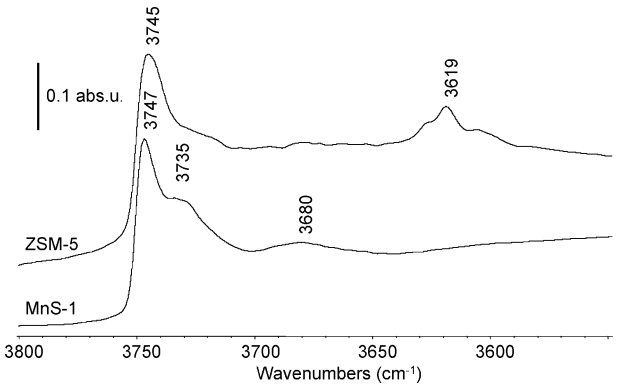


**Figure 11.** IR spectra of the activated, template-free MnS-1 and ZSM-5 in the $\nu$(OH) vibration region.

**3.6. Acidity of MnS-1.** The spectra of template-free, activated MnS-1 and ZSM-5 (Si/Al = 320, ZEOCAT) in the region of the $\nu$(OH) vibrations are presented in Figure 11. Four peaks are present:

(1) 3745−3747 cm$^{-1}$: The peak is evident in the spectra of both samples and is characteristic of $\nu$(OH) vibration of the surface silanols.

(2) 3735 cm$^{-1}$: This peak was assigned to zeolitic silanols that are only accessible via the micropore system and therefore denoted as internal silanols.[29] These silanols correspond to structure defects but do not lead to the formation of so-called silanol nests. The strong intensity of these OH absorption bands on the MnS-1 suggests that silanols were located close to manganese atoms.

(3) 3680 cm$^{-1}$: The weak peak could be assigned to adsorbed water. It is present in MnS-1 after thermal treatment under vacuum. Thus, we assume that it belongs to occluded water molecules and/or to water molecules coordinated to the $Mn^{3+}$, thus leading to Mn−OH vibrations.

(4) 3619 cm$^{-1}$: This peak is only observed in the ZSM-5. It is assigned to the $\nu$(OH) vibration of the acidic bridging OH, which is the compensation for the charge deficit caused by the incorporation of $Al^{3+}$ cations in the framework.

Carbon monoxide is a well-established probe molecule for the characterization of the acidity of solids. Its adsorption at low temperature (∼100 K) on oxide-based materials leads to the formation of H-bonds on Brønsted acid sites.[30−32] When this H-bond is formed, the $\nu$(OH) vibration band is perturbed and shifted to lower wave-

(28) Aranda, M. A. G.; Attfield, J.-P.; Bruque, S. *Inorg. Chem.* **1993**, *32*, 1925.

(29) Thibault-Starzyk, F.; Vimont, A.; Gilson, J. P. *Catal. Today* **2001**, *70*, 229.

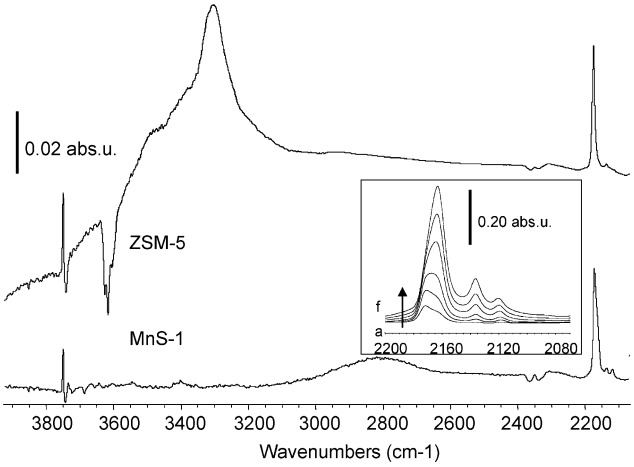


**Figure 12.** IR spectra of template-free MnS-1 and ZSM-5 obtained after CO adsorption at 100 K. Inset: adsorption of increasing doses of CO (from a to f) on MnS-1. Difference spectra are presented here; i.e., the spectrum of the clean activated solid is subtracted.

numbers. The corresponding $\Delta\nu$(OH) shift indicates the strength of the H-bond and thus the strength of the acid site. The $\nu$(CO) vibration band of adsorbed CO is also shifted (but to higher wavenumbers) from its pseudo-liquid frequency at 2138 $cm^{-1}$, and its shift also corresponds to the strength of the perturbation. Precise scales for the acidity of solids have been published.[31] Adsorption on Lewis sites or on cations leads to specific $\nu$(CO) vibration frequencies, which can be used for the identification of the adsorption site.[32] CO has several advantages over other probe molecules: it is a very small molecule and can easily access most of the sites in the framework. Moreover, it can indicate simultaneously the type, strength, and amount of adsorption sites and has sometimes been denoted as "the ideal" probe molecule for the acidity of oxides,[30] with the only drawback of needing liquid nitrogen temperature. Recently, we have successfully used it for the analysis of FeAPO materials.[33]

We applied the carbon monoxide adsorption to assess the presence of Brønsted or Lewis sites on the MnS-1 material and to compare these sites with those observed on the reference ZSM-5 sample (Figure 12):

(1) The formation of H-bond in ZSM-5 produces a negative peak in the difference spectra due to the perturbation of the $\nu$(OH) vibration at 3600−3650 $cm^{-1}$, and a broad positive band centered at 3300 $cm^{-1}$ due to the vibration of the perturbed acidic OH groups (Figure 11). There are no indications for the presence of H-bonds in the MnS-1 sample.

(2) For both materials, a positive/negative pattern is visible on the difference spectra at the frequency of the silanol groups. They appear due to a temperature drift in the cell upon introduction of the first doses of CO and due to a slight blue shift of the $\nu$(SiO−H) vibration band.

(3) A broad peak appears in the spectrum of MnS-1 around 2800 $cm^{-1}$. It corresponds to the perturbation of a combination band of the structure vibrations.

(4) Four bands are observed in the $\nu$(CO) region for CO adsorbed at 100 K on MnS-1 at 2175, 2163, 2138, and 2120 $cm^{-1}$. The 2138-$cm^{-1}$ band is due to physisorbed CO. The bands at 2175 and 2120 $cm^{-1}$ appear on the sample as soon as the first doses of CO are introduced. They are generally assigned to $Mn^{2+}$−CO species.[32] When the amount of CO adsorbed increases, these two bands rapidly reach their maximum. Finally, the band at 2163 $cm^{-1}$ appears, rapidly reaching the strongest intensity. We ascribe this band to $Mn^{3+}$−CO species. We should mention that the $Mn^{3+}$−CO complexes have been found to be unstable at room temperature due to the redox properties of $Mn^{3+}$ inside Mn/$TiO_2$.[34] However, no low-temperature adsorption has been reported so far, despite several reports on room-temperature adsorption of CO on $Mn^{3+}$ cations.

The low-temperature adsorption experiment indicates the presence of $Mn^{3+}$ and $Mn^{2+}$ cations. XANES analysis showed that at least 90% of Mn was 3+. Therefore, it seems reasonable that the intense band obtained at 2163 $cm^{-1}$ was due to $Mn^{3+}$−CO species, which are stable at liquid nitrogen temperature.

The additional check for Brønsted sites in the MnS-1 sample was done by 2,6-lutidine adsorption at the end of the experiment. 2,6-lutidine is more sensitive than pyridine to weak Brønsted sites, but no Brønsted sites were detected.

Finally, we checked the redox behavior of activated MnS-1 sample by doing thermal treatment under hydrogen. No difference could be noticed by comparing the results of CO adsorption at low temperature on oxydized and reduced samples. This fact shows that no redox sites are present in MnS-1.

## 4. Conclusions

We synthesized the manganese-containing silicalite-1 MnS-1 and showed that the manganese isomorphously substituted silicon in the framework. The EXAFS and XANES analyses revealed that at least 90% of manganese in the template-free sample was $Mn^{3+}$, which was also confirmed by IR spectroscopic measurements of CO adsorption/desorption. FT-IR spectroscopic studies of CO adsorption at 100 K on MnS-1 revealed the Lewis acidity of the MnS-1 and the presence of both $Mn^{3+}$ and $Mn^{2+}$ cations in the lattice.

**Acknowledgment.** We are thankful for the support by the Slovenian Ministry of Education, Science and Sport through the research program P0-0516-0104 and the project Z2-3457-0104, by a European PROTEUS project 02629NB, by Internationales Buero BMBF (Germany), and by the IHP-Contract HPRI-CT-1999-00040 of the European Commission. Advice on beamline operation by Konstantin Klementiev of HASYLAB is gratefully acknowledged, as well as help with the infrared experiments by Alexandre Vimont.

CM031091C

(30) Knözinger, H. In *Elementary Reaction Steps in Heterogeneous Catalysis*; Joyner, R. W., Van Santen, R. A., Eds.; Kluwer Academic Publishers: Dordrecht, The Netherlands, 1993.

(31) Cairon, O.; Chevreau, T. *J. Chem. Soc., Faraday Trans.* **1998**, *94*, 323.

(32) Hadjiivanov, K. I.; Vayssilov, G. N. *Adv. Catal.* **2002**, *47*, 307.

(33) Ristic, A.; Tušar, N. N.; Arčon, I.; Logar, N. Z.; Thibault-Starzyk, F.; Czyzniewska, J.; Kaucic, V. *Chem. Mater.* **2003**, *15*, 3643.

(34) Kantcheva, M.; Kucukkal, M. U.; Suzer, S. *J. Catal.* **2000**, *190*, 144.